Science Bulletin 64 (2019) 232–235

Contents lists available at ScienceDirect

Science Bulletin

journal homepage: www.elsevier.com/locate/scib

Science Bulletin
www.scibull.com

Short Communication

Controlling the reaction kinetics in solution for uniform nanoshells of metal sulfides with sub-nanometer accuracy

Shu-Yi Duan [a,b], Zi-Xiao Wu [a,b], Jun-Yu Piao [a,b,c], De-Shan Bin [a,b], Yong-Gang Sun [a,b], Xi-Jie Lin [a,b], An-Min Cao [a,b,*], Li-Jun Wan [a,b]

[a] CAS Key Laboratory of Molecular Nanostructure and Nanotechnology, and CAS Research/Education Center for Excellence in Molecular Sciences, Institute of Chemistry, Chinese Academy of Sciences (CAS), Beijing 100190, China
[b] University of Chinese Academy of Sciences (UCAS), Beijing 100049, China
[c] Institute of Chemical Materials, China Academy of Engineering Physics, Mianyang 621900, China

ARTICLE INFO

Article history:
Received 16 January 2019
Received in revised form 28 January 2019
Accepted 29 January 2019
Available online 10 February 2019

Core-shell nanostructures have found broad potentials in a large variety of applications including catalysis, biomedicine, and energy conversion/storage devices [1,2]. The unique structural configuration endows the composite a capability to combine advantages of both core and shell materials, and deliver optimized properties through a rational design of the components [3]. Accordingly, numerous research efforts have been directed to the synthesis control of the coating materials to build desired nanoshells. Particularly, silica-based core-shell structures have witnessed enormous success benefiting from the flexible synthesis capability ensured by the Stöber process, which provides favorable growth kinetics in solution to build precise configuration of silica nanoshells suited for their applications, for example, silica-based nanocapsules for controlled drug delivery [4].

Transition metal sulfides (TMSs) have attracted increasing research attention for their potential in energy and photonic related applications [5], typically, as anode materials in sodium ion batteries (SIBs) [6]. Significant research efforts have been exerted to the compositional control and structural engineering of TMSs, among which core-shell nanostructures have been widely resorted to combat the sluggish sodiation/desodiation process of TMSs by coating TMSs onto highly conductive substrates [7]. For the TMSs coating efforts, hydro/solvothermal reactions has dominated the synthesis routes, but these high pressure and high temperature conditions inevitably lead to fast precipitation and crystallization of TMSs particles, according forming mainly disordered surface aggregates, in most cases randomly-stacked nanosheets, rather than conformal TMSs nanoshells suited for a systematic surface engineering in both thickness and composition [8]. The technique of atomic layer deposition (ALD) emerges as a powerful tool to resolve this synthetic challenge, which shows a capability to form conformal TMSs coating with high accuracy [9]. Unfortunately, ALD requires expensive machinery and is meanwhile struggled by its limited processing capability, risky precursor chemistry, and tedious operations [10]. It is highly favorable to develop solution-based synthetic routes with a precise surface control capability similar to the ALD technique.

Herein, we demonstrated a synthetic protocol to build uniform TMSs nanoshells starting from a solution-based route, whose reaction control even at room temperature provided an efficient way to control TMSs thickness with sub-nanometer precision. Using thioacetamide (TAA) as the sulfur reservoir, we were able to modulate its decomposition by controlling the reaction parameters, particularly pH value and additives like hydrazine [11], which facilitated the release of sulfide in solution, forming molybdenum sulfide precipitate in a favorable growth kinetics towards the formation of uniform nanoshells. Such a simple reaction route could be readily expanded to construct nanoshells of a large variety of TMSs with well-defined nanostructures suited for their applications. For example, a composite material prepared by coating cobalt sulfide onto graphene substrate showed promising potential as a high performance anode of SIBs.

Taking the preparation of molybdenum sulfide as an example, aqueous solution of 4 mmol/L sodium molybdate and 29 mmol/L TAA were used as the sources for both molybdenum and sulfur, respectively. Polystyrene (PS) particles (40 mg in weight) were used as seeds for further coating, which were around 500 nm in size with a clean surface according to the transmission electron microscopy (TEM) analysis in Fig. 1a. Upon the addition of 70 mmol/L hydrazine under a weak acid condition (pH around 5), molybdenum sulfide could slowly precipitate at room tempera-

* Corresponding author.
E-mail address: anmin_cao@iccas.ac.cn (A.-M. Cao).

https://doi.org/10.1016/j.scib.2019.02.003
2095-9273/

ture. Fig. 1b revealed the emergence of a 6 nm coating layer around each PS nanoparticle, showing a typically core-shell structure without the formation of independent particles. Moreover, much thicker surface coating could be achieved by reducing the amount of seeds. Fig. 1c showed the formation of 25 nm nanoshells on the PS surface when only 10 mg PS spheres were used. A further reduction to 5 mg could obtain a 50 nm coating layer. The elemental mapping revealed that the major constituents of the shell species were indeed molybdenum and sulfur (Fig. S1 online).

For a representative sample shown in Fig. 1c, the obtained coating layer was amorphous as confirmed by the high-resolution TEM (HRTEM) analysis (Fig. S2a online) and the corresponding fast Flourier transformation (FFT) (Fig. S2b online). Similarly, its X-ray diffraction (XRD) pattern showed no obvious peaks (Fig. S2c online). The X-ray photoelectron spectroscopy (XPS) spectra (shown in Fig. S3 online) was then used to probe the chemical composition as well as the oxidation states of the coated sample. The Mo 3d peaks suggested a chemical valence of Mo(IV) [12] while the S 2p peaks indicated a mixture of both disulfide ion and sulfide ion [13]. Meanwhile, the energy dispersive spectroscopy (EDS) test affirmed a Mo/S ratio close to 1:3 in the surface layer (Table S1 online). All the above-mentioned characterizations suggested the formation of a MoS_3 shell, which have been widely known as an amorphous product from the sulfide precipitation of molybdenum [13].

A further high temperature treatment at 700 °C in an inert atmosphere would turn this amorphous sample into highly crystalline one without damaging the particle shape (Fig. 2a). After sintering, the PS core would be removed and hollow nanospheres formed instead (Fig. 2b). The elemental mapping of some randomly-selected spheres (Fig. 2c and d) showed a uniform distribution of Mo and S on the surface, whose EDS analysis gave a Mo/S ratio of around 1:2 (Table S2 online). The XRD test shown in Fig. 2e confirmed the formation of crystalline 2H-MoS_2 (JCPDS No. 06-0097) [14]. Further HRTEM analysis (Fig. 2f) on the surface exhibited clear lattice fringes with their spacing around 0.64 nm (the (0 0 2) planes of MoS_2). It was therefore concluded that the amorphous MoS_3 would crystallize into MoS_2 through the high temperature transition process.

Such a simple solution-based growth route exhibited favorable growth kinetics to slowly form conformal shells, which effectively circumvented the risk of fast precipitation and crystallization process from the reported hydro-solvothermal process and made it possible to grow surface layers with an unprecedented sub-nanometer accuracy [15]. For example, using multi-walled carbon nanotubes (MWCNTs) as the seeds, we were able to precisely define the coating structure, and build multi-layer MoS_2 nanoshells (as shown in Fig. 2g–i). The thickness of MoS_2 gradually increased from 2 layers, to 3 layers, and to 6 layers, manifesting an atomic-level control capability which had usually been considered as the privilege of the ALD technique (TEM images of MWCNTs and amorphous MoS_3 coated MWCNTs showed in Fig. S4 (online)).

The synthetic protocol was flexible to construct molybdenum sulfide nanoshells around different core materials as shown in Fig. S5 (online). This reaction route could also be readily expanded to the creation of a large variety of TMSs nanoshells. Fig. 3 showed our characterizations on representative products for other transition metals including Co (Fig. 3a–e), Zn (Fig. 3f–j), or a multi-compositional one as $Co_{0.5}Ni_{0.5}$ (Fig. 3k–o). The TEM images combined with their corresponding elemental mapping confirmed the effectiveness of our synthesis in building TMSs nanoshells. As a matter of fact, we found that these metal sulfides were much easier

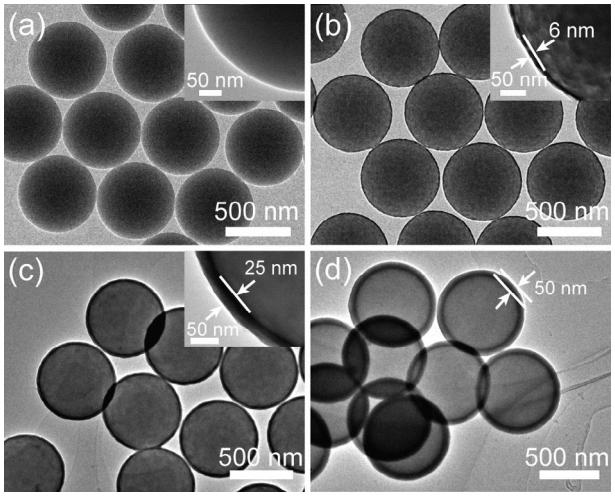

Fig. 1. TEM image of bare PS nanospheres (a) and coated PS nanospheres (b–d). The thickness of molybdenum sulfides coating layer were (b) 6 nm, (c) 25 nm, (d) 50 nm, with different amount of PS seeds and maintained concentration of reactant, 40, 10, and 5 mg, respectively.

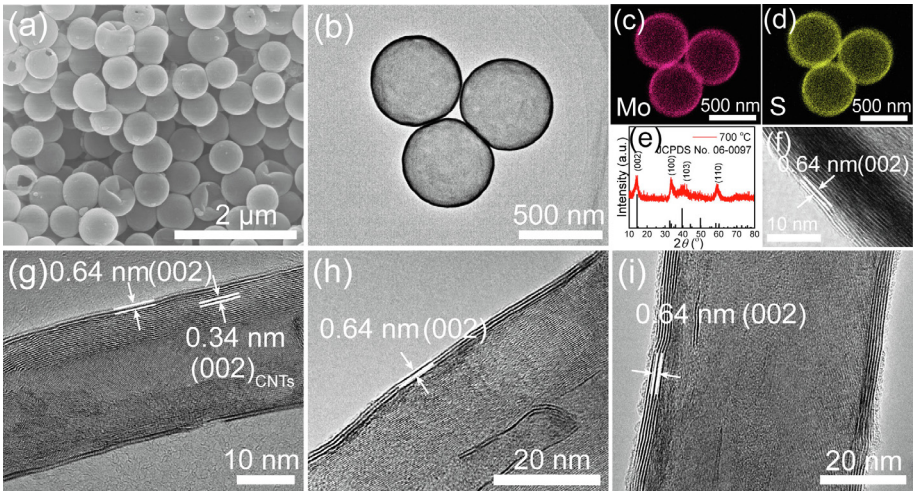

Fig. 2. (Color online) Characterization of hollow MoS_2 nanospheres and MWCNTs@MoS_2. (a) SEM, (b) TEM, (c) and (d) elemental mapping, (e) XRD, and (f) HRTEM results of the prepared hollow MoS_2 nanospheres; **(g–i)** TEM images of core-shell structured MWCNTs@MoS_2 sample with precisely-defined layer numbers of crystalline MoS_2: 2 layers (g), 3 layers (h), and 6 layers (i).

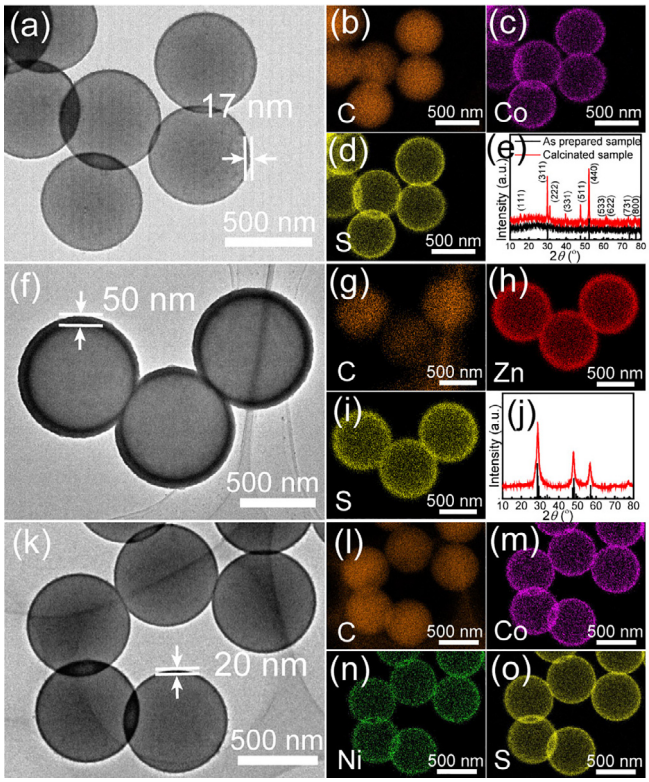

Fig. 3. (Color online) Characterization of various metal sulfide coated PS sample. (a, f, k) TEM images of PS spheres with different metal sulfide coating layers: (a) PS@17 nm CoS_x; (f) PS@50 nm ZnS; (k) PS@20 nm $NiS_x + CoS_x$ (Ni:Co = 1:1). (b–d) Elemental mapping of PS@ CoS_x, (g–i) Elemental mapping of PS@ZnS, (l–o) Elemental mapping of PS@$NiS_x + CoS_x$. (e) XRD patterns of PS@ CoS_x. (j) XRD patterns of PS@ZnS.

to form compared to MoS_3. The pH control alone was effective to produce TMSs coatings without the need of hydrazine as the addictive for TAA decomposition.

The creation of uniform TMSs nanoshells in our synthesis highlighted the effectiveness and flexibility of growth control in solution. Different from those reported synthesis protocols, which usually rely on hydro-solvothermal reactions to initiate the decomposition of sulfur-containing procures, while inevitably endured fast precipitation process to form disordered surface aggregates of TMSs species, our synthesis were inspired by the long-existing and widely-acknowledged observation that the TAA decomposition could be accelerated by hydrazine [16]. Therefore we proposed that the TAA-hydrazine combination would provide a unique tool to modulate the growth kinetics in solution to circumvent the synthesis challenge for TMSs coatings. Our control experiments (Fig. S6 online) clearly demonstrated the critical role played by hydrazine for nanoshell formation. Without the addition of hydrazine, the room temperature reaction could not form any MoS_3 precipitate (Figs. S6a and S6e online). The addition of 30 mmol/L hydrazine made the precipitation of MoS_3 possible (Figs. S6b and S6f online), and this reaction became more evident at 70 mmol/L hydrazine, forming uniform nanoshells as shown in Figs. S6c and S6g (online). Notably, too much hydrazine (150 mmol/L) would enforce a fast precipitation process, and independent MoS_3 particles formed (Figs. S6d and S6h online). We found that the coating process would also be affected by the pH values of the solution, because the TAA decomposition itself was an acid-catalyzed process [11,16]. Detailed experimental results upon pH control were showed in Fig. S7 (online). Through a concerted effort in both hydrazine and H^+ control, it became convenient for us to control the growth of TMSs in solution.

The synthesis protocol reported here has enormous potentials for applications in different research areas such as catalysis, optoelectronics, and energy storage devices. The last of these potentials was demonstrated by using the prepared reduced graphene oxide-Co_9S_8 compound samples (denoted as RGO@Co_9S_8) as an anode material for sodium ion batteries (see the Supplementary Materials for synthesis details, characterizations results in Fig. S8 online). The combination of electrochemically-active TMSs species and conductive graphene matrix was favorable to alleviate the kinetic issue of TMSs anode [17]. Fig. 4a showed the charge/discharge

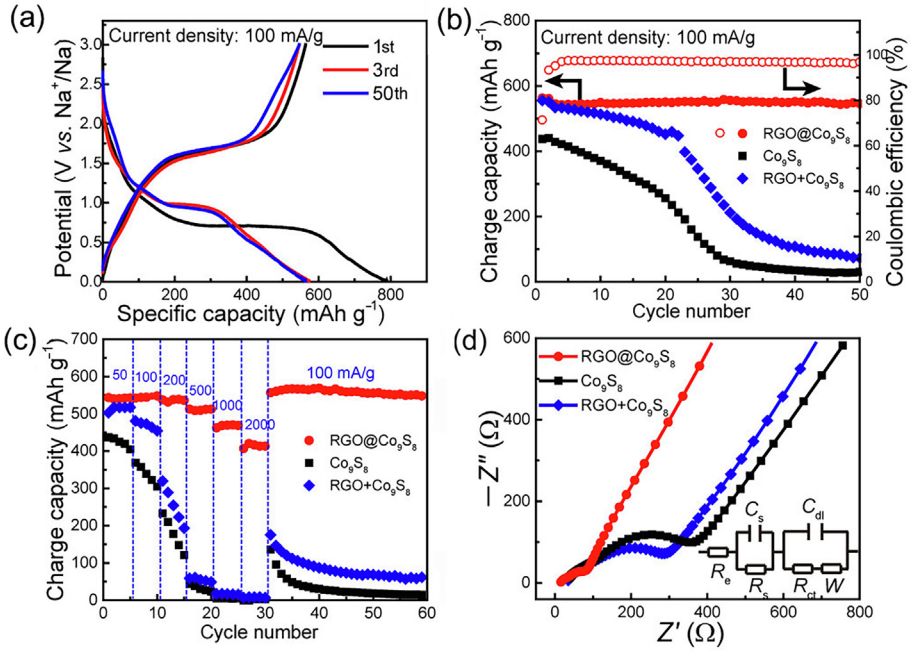

Fig. 4. (Color online) Electrochemical characterization of the core-shell structured RGO@Co_9S_8 and the control samples. (a) Galvanostatic charging/discharging profiles of RGO@Co_9S_8 sample operated at a current density of 100 mA/g from 0.01 to 3.0 V; (b) cycling performance at current density of 50 mA/g for the first two cycles and 100 mA/g for the subsequent cycles; (c) rate performance at current density of 50, 100, 200, 500, 1000, and 2000 mA/g; (d) electrochemical impedance spectrum (EIS).

curves of RGO@Co_9S_8 after different cycles, which showed a high capacity of 553 mAh/g with good reversibility. The much improved cycling capability was further confirmed in Fig. 4b when compared to different control samples. A detailed comparison on the rate capability (Fig. 4c) showed clearly the advantage of the RGO@Co_9S_8 sample especially when working at high rate. The electrochemical impedance spectroscopy (EIS) analysis was carried out to probe the electrochemical kinetics (Fig. 4d) in the assembled cells. The charge transfer resistance of RGO@Co_9S_8 was the smallest among different samples, which was not surprising considering the close electronic contact of the surface metal sulfide and its conductive RGO substrate in RGO@Co_9S_8 (fitting results of EIS was showed in Table S3 online).

We demonstrated a solution-based synthesis strategy to build uniform TMSs coatings with their thickness achieving sub-nanometer accuracy. Using thioacetamide as the sulfur reservoir, we were able to modulate its decomposition by using hydrazine as a unique additive together with the pH control in solution. We identified that the thioacetamide-hydrazine combination provided a highly-efficient tool to modulate the growth kinetics of molybdenum sulfide in solution even at room temperature, and ensured a reliable and versatile process towards the formation of uniform nanoshells instead of highly-crystallized aggregates as prepared from the hydro-solvothermal processes. Such a simple reaction route could be readily expanded to construct nanoshells of a large variety of metal sulfides with well-defined nanostructures suited for their applications.

Conflict of interest

The authors declare that they have no conflict of interest.

Acknowledgments

This work was supported by the National Natural Science Foundation of China (51672282), and the Strategic Priority Research Program of the Chinese Academy of Sciences (XDA09010101).

Author contributions

Prof. A.-M. Cao proposed the experiments; S.-Y. Duan and Z-X. Wu conceived and designed the experiments. S.-Y. Duan and D.-S. Bin performed and analyzed the electrochemical experiments; Y.-G. Sun and X.-J. Lin performed and analyzed the XRD and XPS experiments; S.-Y. Duan and J.-Y. Piao performed and analyzed the TEM and EDS data; Prof. A.-M. Cao and Prof. L.-J. Wan supervised the project; S.-Y. Duan, Prof. A.-M. Cao and Prof. L.-J. Wan wrote the paper. All of the authors discussed the results and reviewed the manuscript.

Appendix A. Supplementary data

Supplementary data to this article can be found online at https://doi.org/10.1016/j.scib.2019.02.003.

References

[1] Bu L, Zhang N, Guo S, et al. Biaxially strained PtPb/Pt core/shell nanoplate boosts oxygen reduction catalysis. Science 2016;354:1410–4.
[2] Wang Y-X, Yang J, Chou S-L, et al. Uniform yolk-shell iron sulfide–carbon nanospheres for superior sodium-iron sulfide batteries. Nat Commun 2015;6:8689.
[3] Ghosh CR, Paria S. Core/shell nanoparticles: classes, properties, synthesis mechanisms, characterization, and applications. Chem Rev 2012;112:2373–433.
[4] Stöber W, Fink A, Bohn E. Controlled growth of monodisperse silica spheres in the micron size range. J Colloid Interface Sci 1968;26:62–9.
[5] Yu XY, Hu H, Wang Y, et al. Ultrathin MoS_2 nanosheets supported on N-doped carbon nanoboxes with enhanced lithium storage and electrocatalytic properties. Angew Chem Int Ed 2015;54:7395–8.
[6] Xiao Y, Lee SH, Sun Y-K. The application of metal sulfides in sodium ion batteries. Adv Energy Mater 2017;7:1601329.
[7] Zhou L, Zhang K, Sheng J, et al. Structural and chemical synergistic effect of CoS nanoparticles and porous carbon nanorods for high-performance sodium storage. Nano Energy 2017;35:281–9.
[8] Wang Y, Yu L, Lou XW. Synthesis of highly uniform molybdenum-glycerate spheres and their conversion into hierarchical MoS_2 hollow nanospheres for lithium-ion batteries. Angew Chem Int Ed 2016;55:7423–6.
[9] Dasgupta NP, Meng X, Elam JW, et al. Atomic layer deposition of metal sulfide materials. Acc Chem Res 2015;48:341–8.
[10] Guo Z, Wang X. Atomic layer depositon of the metal pyrites FeS_2, CoS_2 and NiS_2. Angew Chem Int Ed 2018;57:5898–908.
[11] Haruta M, Lemaitre J, Delannay F, et al. Preparation and porperties of colloidal spherical-particles of molybdenum and cobal sulfides. J Colloid Interface Sci 1984;101:59–71.
[12] Jin B, Zhou X, Huang L, et al. Aligned MoO_x/MoS_2 core-shell nanotubular structures with a high density of reactive sites based on self-ordered anodic molybdenum oxide nanotubes. Angew Chem Int Ed 2016;55:12252–6.
[13] Ye H, Wang L, Deng S, et al. Amorphous MoS_3 infiltrated with carbon nanotubes as an advanced anode material of sodium-ion batteries with large gravimetric, areal, and volumetric capacities. Adv Energy Mater 2017;7:1601602.
[14] Vanchura BA, He P, Antochshuk V, et al. Direct synthesis of mesostructured lamellar molybdenum disulfides using a molten neutral n-Alkylamine as the solvent and template. J Am Chem Soc 2002;124:12090–1.
[15] Liu W, Lei C, Zhang H, et al. CuS/RGO hybrid by one-pot hydrothermal method for efficient electrochemical sensing of hydrogen peroxide. Chin Chem Lett 2017;28:1306–11.
[16] King DM, Anson FC. Use of hydrazine to accelerate the rate of hydrogen sulfide evolution from thioacetamide solutions. Anal Chem 1961;33:572–5.
[17] Lu Y, Chen J. Robust self-supported anode by integrating Sb_2S_3 nanoparticles with S, N-codoped graphene to enhance K-storage performance. Sci China Chem 2017;60:1533–9.

Shu-Yi Duan is a Ph.D. candidate in Key Laboratory of Molecular Nanostructure and Nanotechnology, Institute of Chemistry, Chinese Academy of Sciences (ICCAS). Her research interest mainly focuses on designing and constructing core-shell structured materials for sodium ion batteries.

An-Min Cao earned his Ph.D. degree from the Institute of Chemistry, Chinese Academy of Sciences (ICCAS) in 2006. He worked in Prof. Götz Veser's group on industrial catalysis during 2007–2010. After two more years' postdoctoral research at the University of Texas at Austin with Prof. Arumugam Manthiram on lithium ion batteries, he started his current position as a PI in ICCAS in 2012. His research currently focuses on the surface and interface control of electrode materials for different battery systems.